



## Nanoscale

### REVIEW ARTICLE

**Table 1 Nanotopographies generated by different Top-Down fabrication techniques**

<b>Fabrication Method</b>	<b>Topography</b>	<b>Feature Size</b>	<b>Reference</b>
<b>Electron Beam Lithography</b>	Nanopits	120nm diameter, 100nm depth, 300nm centre to centre spacing	229
	Nanodots	12nm dots with 25nm period and 20nm lines with 40nm period	230
<b>Photolithography</b>	Micropatterns	1-2 $\mu$ m	231
	Micropatterns	1, 5 and 10 $\mu$ m steps	232
	Nanogratings	600nm	96
<b>Phase Separation</b>	Nanodots	20nm dots with 40nm periods	119
	Random Nanofiber	50-500nm	120
	Worm-Like and Dot-like Patterns	160nm	121
	Nanoislands	13, 35 and 95nm high	122
<b>Anodization</b>	Nanotubes	30-100nm	233
	Nanopillars	15-100nm	234
	Nanotubes	15-100nm	235, 236

**Table 2 Nanotopographies generated by different Bottom-Up fabrication techniques**

<b>Fabrication Method</b>	<b>Topography</b>	<b>Feature Size</b>	<b>Reference</b>
<b>Colloidal Lithography</b>	Nanocolloids	20nm diameter particles, 60nm mean interparticle distance.	237
	Nanoislands	120-600nm diameter	in 238
	Nanopillars	50-90nm diameter and 20nm high	in 239
	Nanocolloids	20-500nm	240
	Nanoarrays	100nm	241
<b>Reactive Ion Etching</b>	Random roughness	1-150nm	242
<b>Electrospinning</b>	Random and aligned nanofibers	369-554nm	243
	Random nanofibers	200-400nm	244, 245
	Nanofibers	400-800nm	246
	Nanofibers	350-1100nm	247
	Random and aligned nanofibers	196-253nm	248
<b>Nanoimprinting</b>	Nanopits	50nm	249
	Nanogrooves	350nm	250
	Nanogratings	350-1000nm width	251
<b>Replica Moulding</b>	Nanopillars	400 and 700nm	252

**Table 3 Effects of surface nanotopographies on immunomodulation**

Topography	Feature Size	Modification on surface properties	Immunomodulatory effects	Reference
<b>Nanotubes</b>	~170 nm in diameter, 1 $\mu$ m in length	Roughness: Ra 667.33 nm Contact angle: 25.8°	Reduced inflammatory response	175
	30 nm and 80 nm TiO <sub>2</sub> nanotube surface	Contact angle: polished surface > 30 nm > 80 nm	Enhanced the attachment of macrophages, while inhibited expression inflammatory cytokines, including TNF- $\alpha$ , MCP-1 and MIP-1 $\alpha$	176
	TiO <sub>2</sub> nanotube surface structures with different diameters (30, 50, 70, and 100 nm)		Nanotube surfaces with 70 nm diameter produced the weakest inflammatory response	177
<b>Nanopits</b>	Nanopits (100-nm deep, 120-nm diameter) on 8% 3-hydroxyvalerate-component (D400G)		At 72 h, no significant change in IL-1 $\beta$ , while downregulation observed in the expression of IL-6 and TNF $\alpha$ , compared with D400G without nanopits structure; At day 7, slight downregulation observed in IL-1 $\beta$ and TNF $\alpha$ , with no significant change in IL-6.	181
<b>Nanofibers</b>	~270 nm in diameter, pore size 480 nm	Indentation elastic modulus: 348 Mpa Tensile elastic modulus: 6.81 Mpa	Reduced inflammatory response; switch macrophages to M2 extreme.	186
	sP(EO-stat-PO)-coated hydrogels and PLGA coated 2D substrates as well as 3D nanofiber	Contact angle: hydrogel+nanofiber too hydrophilic for contact angle determination; PLGA+nanofiber 120°	Switch macrophages to M2 extreme	185
<b>Nanodots</b>	10-200 nm Nanodots array		The expression of inflammatory genes was upregulated for the 100- and 200-nm surfaces in macrophages and foam cells.	184
<b>Nanorods</b>	ZnO nanorod surface, nanorod diameter is ~50 nm and height is ~500 nm.		Reduced adhesion number of macrophages, while maintaining their viability	188

<b>Nano-cylinders</b>	Nanocylinders (160-nm height, 100-nm diameter) on the PCL surface	At 72 h, no significant change in IL-1 $\beta$ and IL-6, while downregulation observed in the expression of TNF $\alpha$ , compared with PCL without nanocylinders structure; At day 7, downregulation observed in TNF $\alpha$ , with slight upregulation in IL-6 and IL-1 $\beta$ .	181
<b>Nanopores</b>	Alumina membrane, pore sizes 20, 200 nm	Stronger inflammatory response of macrophages in 200 nm nanoporous structure.	196
	Alumina membrane, pore sizes 20, 200 nm	Neutrophils attached and extended better in 20 nm membrane, with stronger initial oxygen free radical production.	197
<b>Nano-grooves</b>	Nanopatterned polystyrene substrates Groove depth 32.7-158 nm; Ridge 71.9-536.4 nm	At day 1, gene expression of IL-1 $\beta$ was upregulated, while that of IL-10 was downregulated and no significant change was observed in TNF $\alpha$ ; At day 3, gene expression of IL-1 $\beta$ and TNF $\alpha$ was upregulated, while no significant change was observed in IL-10	193
	Nanogroove generated by aligning carbon nanotubes in a polymer matrix; groove width: 100, 60, 30 $\mu$ m	Compared with polymer matrix, surface roughness and energy increased	192

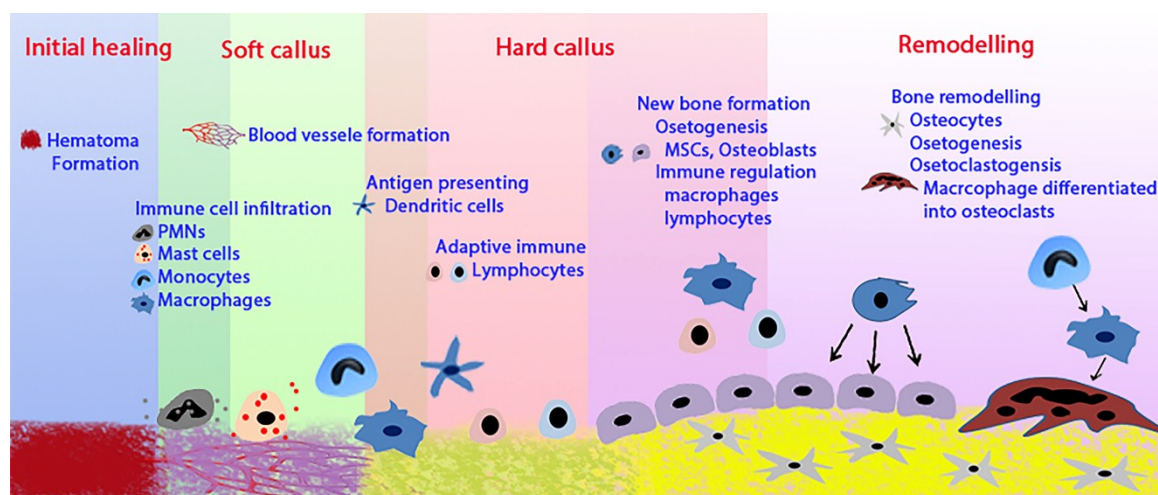


**Figure 1.** The involvement of immune cells on bone healing process. Immune cells participate in all four healing stages. During initial healing stage, immune cells including neutrophils, mast cells, and monocytes/macrophages infiltrate soon after the formation of hematoma. Acute inflammation occurs spontaneously, generating an immune environment favouring angiogenesis and further osteogenesis. New blood vessels are formed, supplying demand nutrients for bone formation and remodelling. Adaptive immune response also involves. Dendritic cells present local antigens to lymphocytes, thus activating adaptive immune response, to further regulate the immune environment for healing to progress. During new bone formation, bone forming cells following the signals from immune cells, to elicit the osteogenic differentiation and bone matrix deposition. The osteoimmune environment also determines the balance of osteogenesis and osteoclastogenesis, regulating the timely bone formation and remodelling. Immune cells play indispensable roles in the bone healing process.

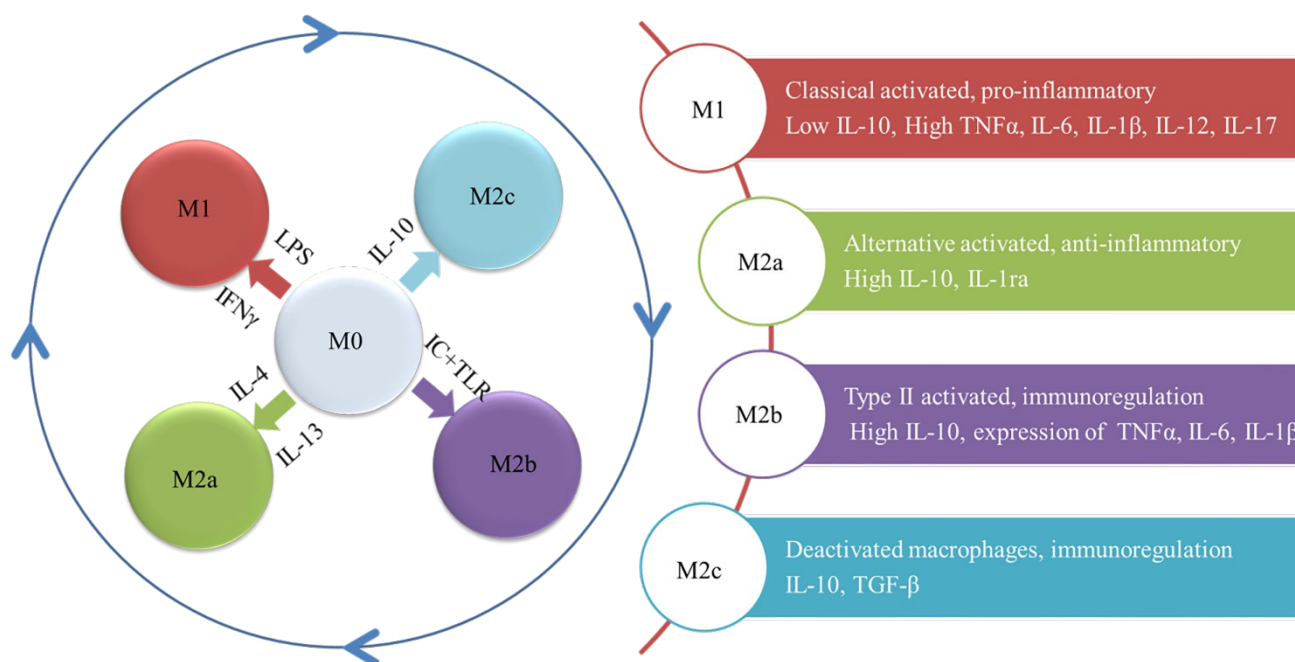


**Figure 2. Plasticity of macrophages. Macrophages have different phenotypes, M1, M2a, b, c. In response to different inducers, macrophages can switch their phenotypes for adaption. This switch is not permanent, but can change back to M0 or other phenotypes depending on the stimulators. Each phenotype has their feature immune functions. This implies the high plasticity of macrophages and its potential in generating different immune environment.**

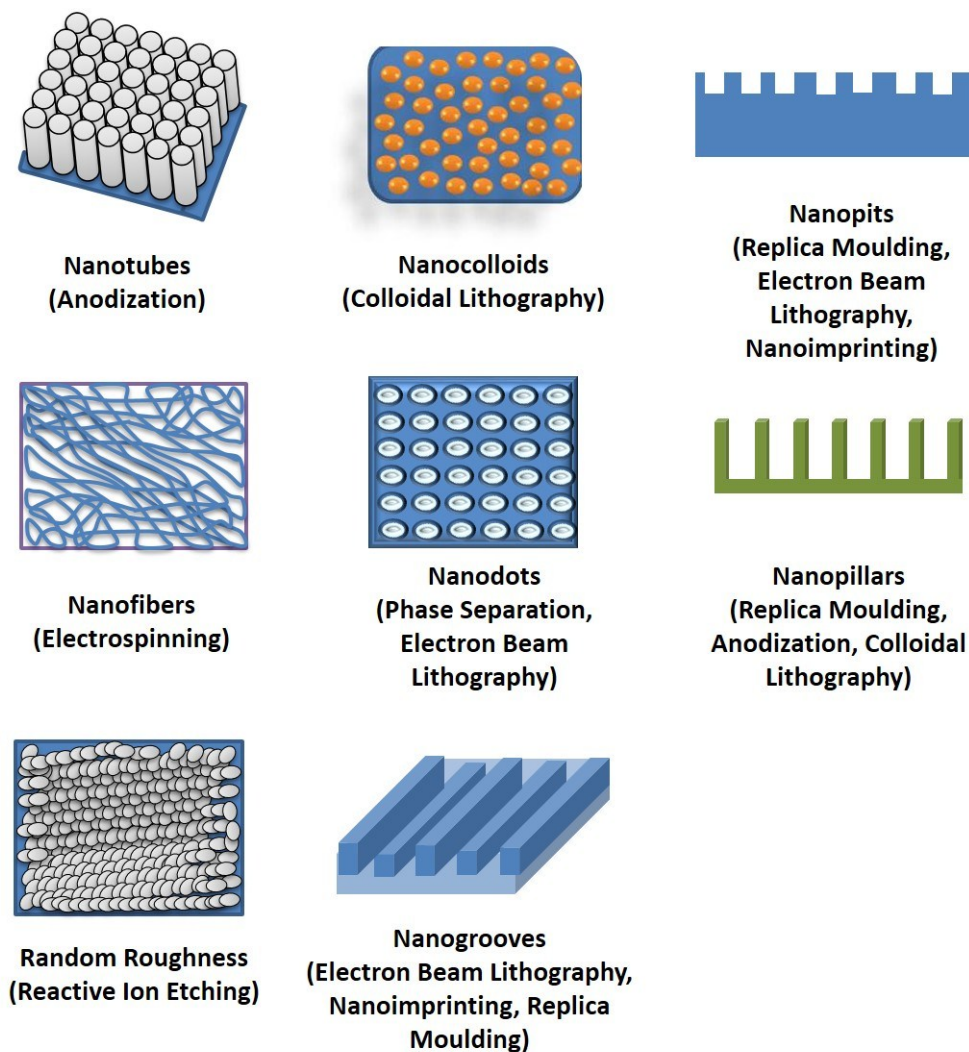


**Figure 3.** Schematic figure of typical nanostructures used for bone regeneration applications.

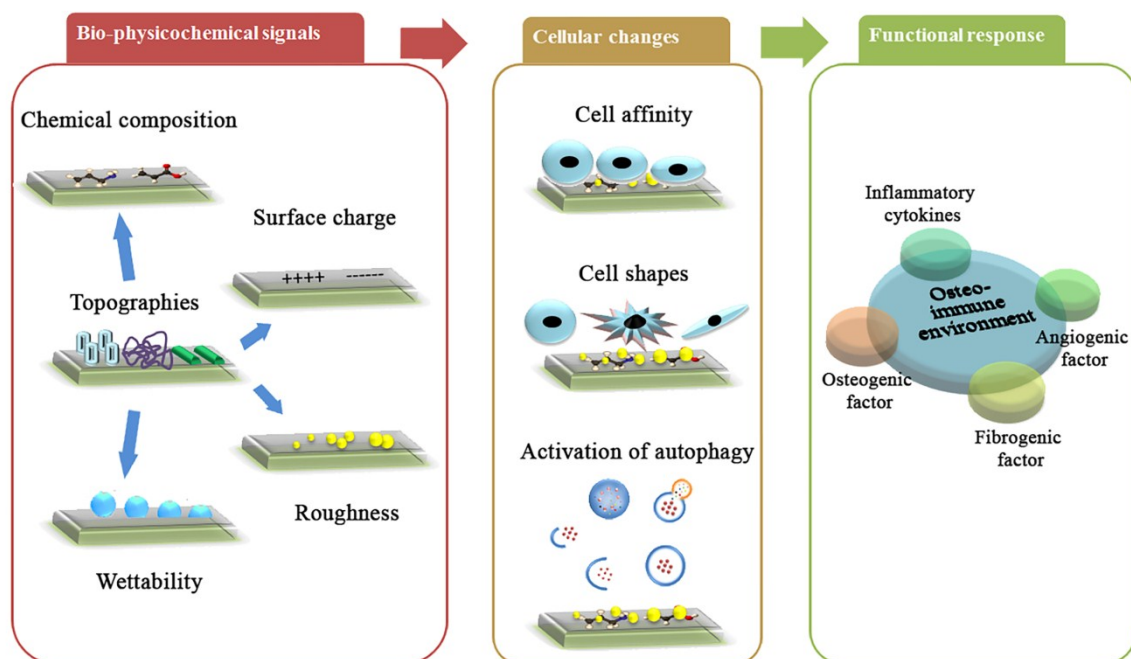


**Figure 4.** Immunomodulatory effects of different nanotopographies. Many types of nanotopographies, including nanotubes, nanopits, nanofibers, nanodots, nanorods, nanogrooves and nanopores, have been applied for bone biomaterials applications. Each type of nanotopography has its unique bio-physicochemical and mechanical properties. *Via* changing relating parameters, these properties can be effectively modified, thus generating various bio-physicochemical and mechanical signals. In response to these signals, immune cells with high plasticity adapt promptly, translating the signals into biological response. The underlying mechanisms could be related to the protein absorption profiles, thus affecting cell attachment, shapes, and activation of autophagy intracellular. Eventually, the modulated effects reflect in the functional response of immune cells, resulting in different micro-immune environment.

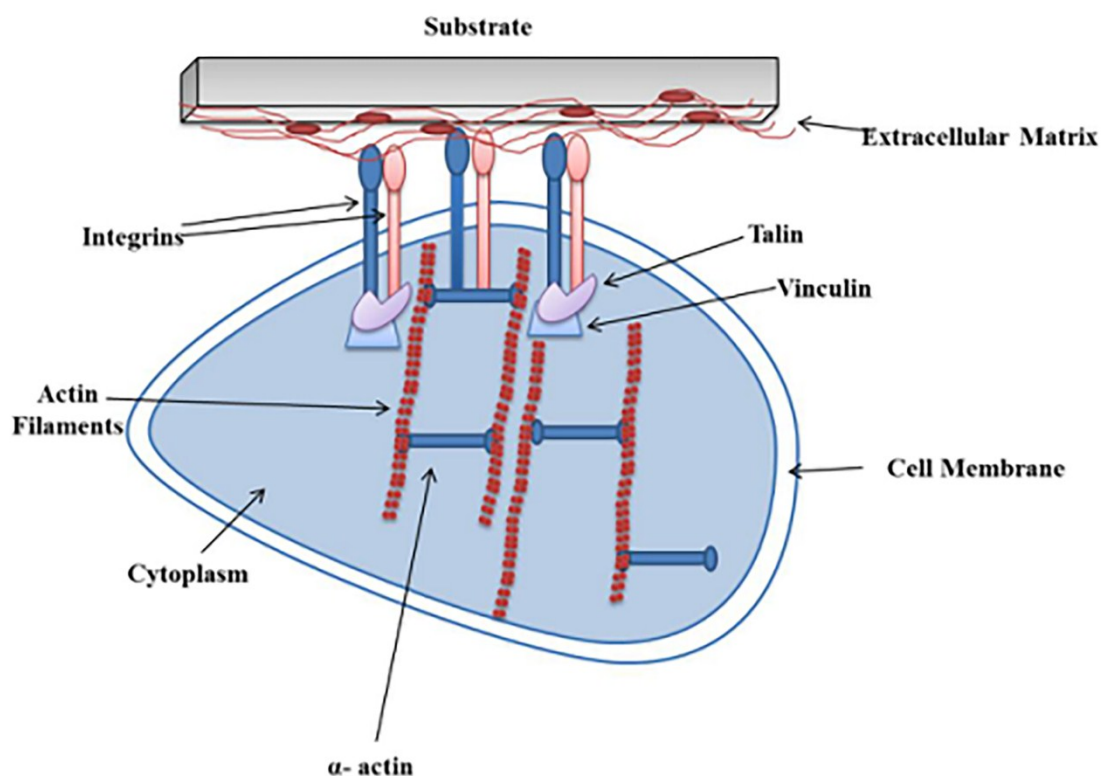


**Figure 5. Cells-surface interaction.** Cell adhere to the surface *via* integrins on cell surfaces to the adsorbed proteins on the material surface. Cell-receptor ligation takes place within ECM, leading to the initiation of integrin clustering at the cell membrane. After attachment, ECM interacts with the actin filaments *via* adaptor proteins such as talin and vinculin. This helps the cell to investigate the physical properties of ECM and change the cell shape based on gathered information.

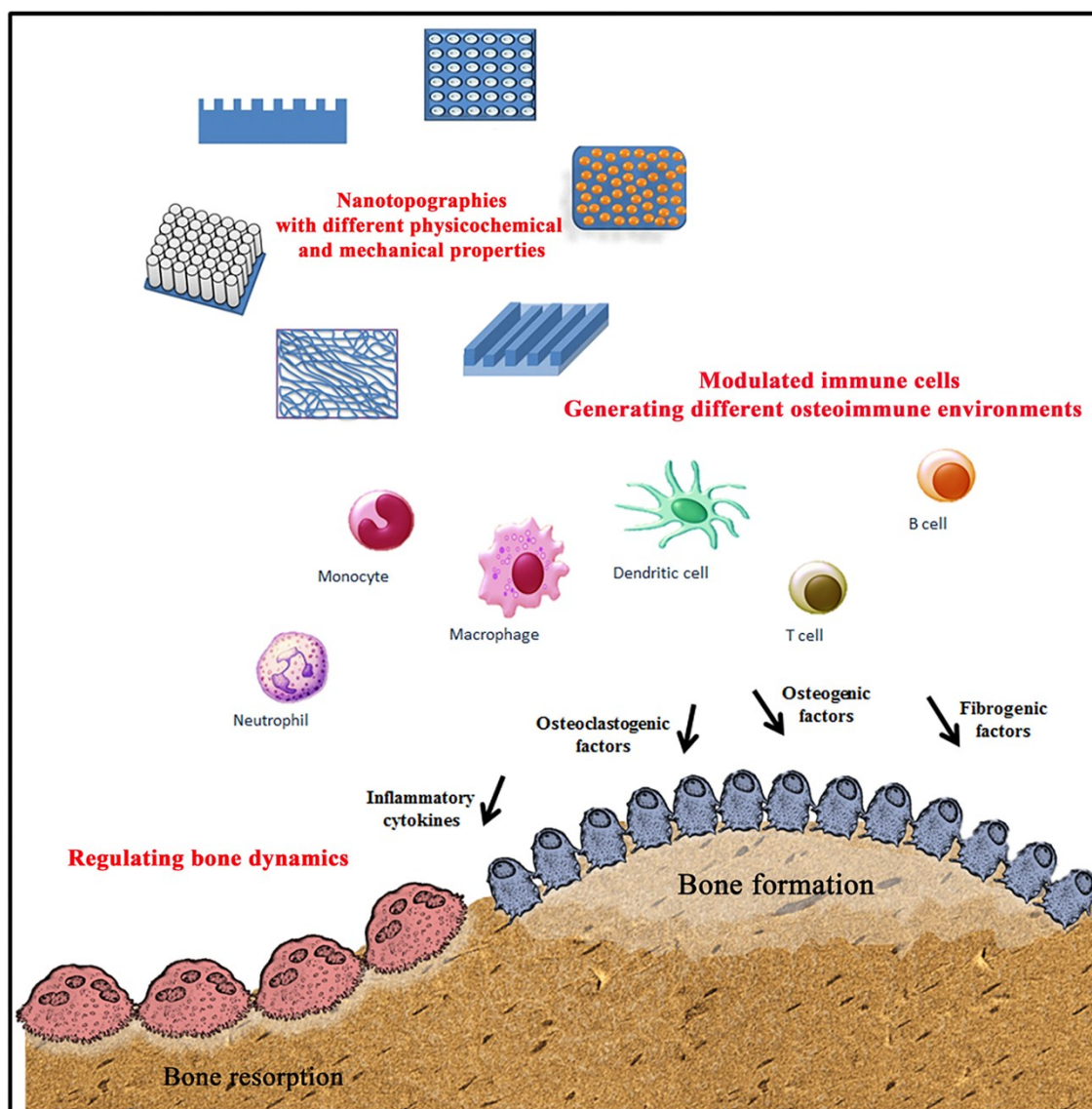


**Figure 6.** Nanotopography-based strategy to manipulate osteoimmunomodulation. *Via* modifying the biophysicochemical and mechanical properties of nanotopography, the immune response can be effectively modulated, thus generating different osteoimmune environments. Under the regulation of these environments, bone dynamics would be significantly changed, affecting the balance of osteogenesis and osteoclastogenesis and determining the regeneration outcomes. (partially adapted from <sup>253</sup>)

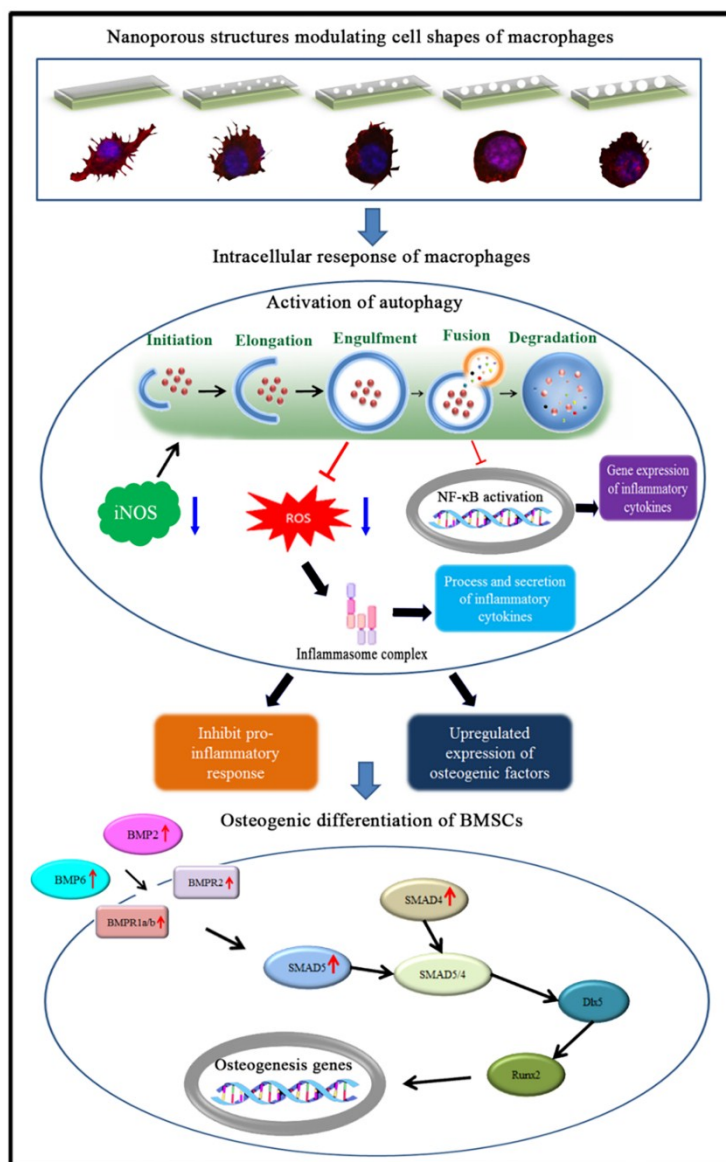


**Figure 7.** The osteoimmunomodulatory effects of nanotopographies on macrophages. In response to the bio-physicochemical signals from the nanotopographies, macrophages change their shape, leading to intracellular environmental changes. To maintain intracellular homeostasis, autophagy is activated, which induces the production of ROS that interact with inflammasome complexes (promoting the maturation and release of the inflammatory cytokines IL-1 $\beta$  and IL-18), resulting in the release of pro-inflammatory cytokines. In addition, autophagy can also modulate NF- $\kappa$ B (an important transcriptional factor for pro-inflammatory cytokine genes) activation, impeding the expression of pro-inflammatory cytokine genes. Stimulated macrophages also release osteogenic factors, including BMP2/6, which lead to the activation of the BMP pathway in BMSCs and the enhancement of osteogenic differentiation (Adapted from ref. 198 with permission from the Royal Society of Chemistry <sup>198</sup>).